FEM For Nernst-Planck-Poisson Equation

ME5204 Finite Element Analysis (course project)

Jay Prajapati, Yash Panasara

Department of Mechanical Engineering,
Indian Institute of Technology Madras, Chennai - 600036, India.
me21b143@smail.iitm.ac.in, me21b135@smail.iitm.ac.in

Abstract

The Nernst-Planck-Poisson (NPP) system of equations is a widely employed framework for analyzing ion diffusion mechanisms in materials integral to storage batteries and solid oxide fuel cells. Specifically, the NPP equations facilitate the prediction of charged defect concentrations and electric potential distributions. These distributions often exhibit steep gradients near the boundaries, particularly in computational domains of significant size. In this study, the traditional finite element method (FEM) is utilized to solve the NPP equations. To accurately capture the boundary gradients, a refined mesh strategy is employed, leveraging the simplicity of polynomial-based approximations inherent to FEM.
Keywords: Nernst-Planck-Poisson equations, Mixed ionic-electronic-conductor, Steep gradient

1 Introduction

The Nernst-Planck-Poisson (NPP) system is a mathematical framework that describes the transport of charged species, such as ions and electrons, within electrolytic solutions under the influence of an electric potential. It provides a mean-field approximation of ion interactions and a continuum representation of concentration and electrostatic potential. The NPP equations offer both qualitative insights and quantitative predictions for experimental observations in ion transport phenomena. These equations are derived from the foundational principles of electrochemistry and electrostatics.

The Nernst-Planck-Poisson (NPP) system has broad applicability in analyzing the conduction of charged entities across diverse domains, including semiconductors [1, 2], biological systems [3, 4], and electrochemistry [5]. It represents a coupled framework integrating the Nernst-Planck and Poisson equations. The Nernst-Planck equation extends Fick's first law by accounting for the influence of an electric field on the flux of charged particles. The Poisson equation establishes the relationship between charge distribution and the electric potential generated by the charged species within the system, thereby encapsulating the coupling dynamics of these species.

In solving the Nernst-Planck (NP) equation, several assumptions are typically made. Two of the most commonly used assumptions are constant electric field and electroneutrality. However, the results derived from these assumptions do not satisfy the Poisson equation. Specifically, under the assumption of a constant electric field, the charge density must be zero everywhere. Conversely, assuming electroneutrality leads to a constant electric field. While these assumptions may hold true in the bulk of the domain, they fail to accurately describe the system at the boundaries and interfaces.

The Nernst-Planck-Poisson (NPP) equations were initially introduced by Eisenberg and colleagues [6, 8] to model ion transport in membrane channels. The theoretical framework supporting the existence of a solution for the steady-state NPP equations has been established by Jerome [9] and Hayeck et al. [10] using the Schauder fixed point theorem. Due to the presence of permanent charges, the electrostatic potential, as well as the ionic concentration and its gradients near the molecular surface, exhibit significant magnitudes. These gradients become even steeper as the domain size increases. The high degree of non-linearity and strong two-way coupling in the system makes the solution of the NPP equations particularly challenging. Consequently, most of the methods used to solve these equations in the literature are numerical, with only a few attempts at analytical solutions. The prevalent numerical approaches include perturbation methods, finite difference methods, finite volume methods, and the finite element method.

In this study, we focus on employing the traditional Finite Element Method (FEM) to solve the Nernst-Planck-Poisson (NPP) equations, specifically to capture the steep gradients near the boundary. The accuracy of the proposed solution is evaluated through one-dimensional examples with appropriate boundary conditions. The paper first discusses the governing equations and their weak form, followed by an explanation of the shape functions and the numerical integration scheme used. A mesh convergence study is then presented to assess the accuracy of the solution with respect to mesh refinement. Finally, the results are interpreted, and conclusions are drawn based on the findings.

2 Governing equations and boundary conditions

The Nernst-Planck-Poisson equation combines electric and chemical behaviour to analyse charged species's diffusion and describes the ionic flux in a solution under the influence of electric potential, which is expressed as:

$$j_i = -D_i(\nabla c_i + \frac{z_i F}{RT} c_i \nabla V) \qquad i = \{1, 2, .., ns\} \tag{1}$$

where ns is the number of species, j_i is the diffusion flux, c_i is the concentration (mol m^{-3}), z_i is the valency, D_i is the diffusion coefficient ($m^2 s^{-1}$) of ith species, T is the temperature (K), R is the universal gas constant ($Jmol^{-1}K^{-1}$), F is the Faraday's constant (A s mol^{-1}), V is the electric potential (V) and ns is the number of species. The law of conservation of mass for each ionic species is given by:

$$\frac{\partial c_i}{\partial t} + \nabla \cdot j_i = 0 \qquad in \;\; \Omega \tag{2}$$

Substituting Eq. (1) into Eq. (2), we get Nernst-Planck equation:

$$\frac{\partial c_i}{\partial t} + \nabla \cdot (-D_i(\nabla c_i + \frac{z_i F}{RT} c_i \nabla V)) = 0 \qquad in \;\; \Omega \tag{3}$$

For the case of One-dimensional, the Nernst-Planck equation simplifies to:

$$\frac{\partial c_i}{\partial t} + \frac{\partial}{\partial x}(-D_i(\frac{\partial c_i}{\partial x} + \frac{z_i F}{RT} c_i \frac{\partial V}{\partial x})) = 0 \tag{4}$$

where c_i and V are the unknown concentration and potential field, respectively. The above mass conservation equation is supplemented with the Poisson equation for the electric potential with the body load the spatial distribution of electric charges, given by:

$$\nabla^2 V + \frac{\rho}{\varepsilon} = 0 \qquad in \;\; \Omega \tag{5}$$

In One-dimensional, the Poisson equation simplifies to:

$$\frac{\partial^2 V}{\partial x^2} + \frac{\rho}{\varepsilon} = 0 \tag{6}$$

where, ρ is the volume charge density, ε is the permittivity of medium. The volume charge density represents the coupling of all the charged species, which is given by

$$\rho = F(\sum_{i=1}^{ns} z_i c_i + \omega) \tag{7}$$

where ω is the fixed charged density over the domain. Eq. (3) and (5) combined is called Nernst-Planck-Poisson equation. These equations are supplemented with appropriate boundary conditions.

Dirichlet boundary conditions:

$$c_i = c_0 \qquad on \quad \Omega_D \tag{8}$$

$$V_i = V_0 \qquad on \quad \Omega_D \tag{9}$$

Neumann boundary conditions:

$$j_i.\widehat{n} = 0 \qquad on \quad \Omega_N \tag{10}$$

$$\nabla V.\widehat{n} = 0 \qquad on \quad \Omega_N \tag{11}$$

where $\widehat{n}$ denotes outward normal vector, $\Omega = \Omega_D \bigcup \Omega_N$ and $\Omega_D \bigcap \Omega_N = \phi$ denoted the domain boundaries and Dirichlet and Neumann conditions respectively.

3 Weak form

To solve the following system of equations using FEM, we will first convert the strong form to weak form. This is obtained by multiplying an arbitrary test function and integrating it over the domain (weight residual method). The weak forms are as follows:-

$$\int_\Omega g_i[\frac{\partial c_i}{\partial t} + \nabla \cdot (-D_i(\nabla c_i + \frac{z_i F}{RT} c_i \nabla V))]d\Omega = 0 \tag{12}$$

$$\int_\Omega v[\nabla^2 V + \frac{\rho}{\varepsilon}]d\Omega = 0 \tag{13}$$

where g_i and v are the test functions for the concentration and potential field respectively. The above equations are integrated over the domain Ω. By applying the Gauss-divergence theorem, along with the assumption of steady-state transportation of charged species, gives,

$$\int_\Omega \nabla g_i \cdot [D_i(\nabla c_i + \frac{z_i F}{RT} c_i \nabla V)]d\Omega + \int_{\partial\Omega} g_i[-D_i(\nabla c_i + \frac{z_i F}{RT} c_i \nabla V)] \cdot \widehat{n} d\partial\Omega = 0 \tag{14}$$

$$-\int_\Omega \nabla v \cdot \nabla V d\Omega + \int_{\partial\Omega} v \nabla V \cdot \widehat{n} d\partial\Omega + \int_\Omega v \frac{F}{\varepsilon}(\sum_{i=1}^{ns} z_i c_i + \omega)d\Omega = 0 \tag{15}$$

where Eqs. (14) and (15) are continuous weak or variational forms over the domain. The domain is discretized into non-overlapping regions called elements, connected at points called nodes. The unknown fields are represented by piecewise polynomials.

The solutions are approximated by these polynomial functions which are represented as follows:

$$c_i = [c_{i1}, c_{i2}, c_{i3}, ..., c_{iN}]^T \tag{16}$$

$$V = [V_1, V_2, V_3, ..., V_N]^T \tag{17}$$

$$g_i = [g_{i1}, g_{i2}, g_{i3}, ..., g_{iN}] \tag{18}$$

$$v = [v_1, v_2, v_3, ..., v_N] \tag{19}$$

$$\phi = [\phi_1, \phi_2, \phi_3, ..., \phi_N] \tag{20}$$

$$B = [\frac{\partial \phi_1}{\partial x}, \frac{\partial \phi_2}{\partial x}, \frac{\partial \phi_3}{\partial x}, ..., \frac{\partial \phi_N}{\partial x}] \tag{21}$$

where N denotes the number of nodes in a element. Upon Substituting these approximated forms in weak forms, the matrix form of weak form can be expressed as:

$$\int_\Omega B^T D_i (B\widehat{c_i} + \frac{z_i F}{RT}\widehat{c_i} B\widehat{V}) d\Omega + \int_{\partial\Omega} \phi^T (j_i \cdot \widehat{n}) d\partial\Omega = 0 \tag{22}$$

$$-\int_\Omega B^T B\widehat{V} d\Omega + \int_{\partial\Omega} \phi^T (\nabla V \cdot \widehat{n}) d\partial\Omega + \int_\Omega \phi^T \frac{F}{\varepsilon} (\sum_{i=1}^{ns} z_i c_i + \omega) d\Omega = 0 \tag{23}$$

The NPP equations are fully coupled and non-linear equations exhibiting singular solutions for a particular choice of ε. These non linear set of equations can be solved by either Picard iteration or Newton Raphson method. Here, we have considered only Picard iteration for simplicity.

4 Choice of Mesh

As we have mentioned so far that we have been solving the One-dimensional version of NPP equations. So, the mesh is also one-dimensional. The mesh is generated by dividing the domain into a number of elements. The number of elements can be chosen based on the complexity of the problem. The mesh is refined near the boundaries to capture the steep gradients. The nodes and elements are represented as follows:

$$nodes = [0, 1, 2, ..., N-1]$$

$$elements = [[0, 1], [1, 2], ..., [N-2, N-1]]$$

The following table summarizes the mesh parameters used in the numerical examples:

5 Shape functions in parametric space

The shape functions are used to approximate the solution in the element. The shape functions are defined in the parametric space. The shape functions are defined as follows:

$$\phi_1 = \frac{1}{2}(1-\xi) \qquad \phi_2 = \frac{1}{2}(1+\xi) \tag{24}$$

where ξ is the parametric coordinate.

Table 1: Physical parameters used in the numerical examples

Physical Quantity	Value
Temperature (T)	873 K
Universal Gas Constant (R)	8.3144 $Jmol^{-1}K^{-1}$
Faraday's constant (F)	96,485.3321 $A\ s\ mol^{-1}$
Permittivity of free space (ϵ)	$8.854 \times 10^{-12}\ F\ m^{-1}$
Dielectric constant	30,000
Diffusion Constant of ion (D_1)	$6.18 \times 10^{-9} m^2\ s^{-1}$
Diffusion Constant of electron (D_2)	$3.89 \times 10^{-7} m^2\ s^{-1}$
Max ion/electron concentration (c_0)	$82,101 mol\ m^{-3}$
Fixed charge density (ω)	$0\ mol\ m^{-3}$
Valency of 1st species (z_1)	+2
Valency of 2nd species (z_2)	-1
Length	1 nm
K_1 (F/RT)	$13.293\ A \cdot s/J$
K_2 (F/(Dielectric constant * ϵ))	3.632×10^{11}

6 Numerical Integration scheme used

The numerical integration scheme used in the FEM is the Gaussian quadrature. The Gaussian quadrature is used to approximate the integrals in the weak form. The number of Gauss points required is dependent on the order of the polynomial to be approximated, which in our case is 2nd order polynomial and hence 2n-1 gauss points i.e. 3 gauss points are required. The Gauss points and weights are given as follows:

$$Gauss\ points = [-\sqrt{0.6}, 0, \sqrt{0.6}] \qquad Gauss\ weights = [\frac{5}{9}, \frac{8}{9}, \frac{5}{9}]$$

7 Mesh Convergence Study

In this section, we present the procedure and results of the mesh convergence study conducted to assess the accuracy of the solution to the Nernst-Planck-Poisson (NPP) equations. The study involves refining the mesh (increasing the number of nodes) and evaluating the resulting errors in the computed variables: potential (V) and concentrations (C_1, C_2).

7.1 Procedure

The study follows the following steps:

1. **Mesh Generation:** Generate a one-dimensional mesh for a range of node counts: {15, 100, 500, 750, 1000, 1250, 1500, 1750, 2000, 2250, 2500}. Define boundary conditions: $V_{\text{left}} = 0$, $V_{\text{right}} = 0.133$, $C_{1,\text{bc}} = C_{2,\text{bc}} = 82101$.

2. **Initialize Variables:** Set initial values for V, C_1, and C_2 across the mesh. Use boundary conditions to fix values at the boundaries.

3. **Iterative Solution:** Assemble the global matrices (L, O, and M) required for solving the NPP equations. Iteratively solve for the potential (V) and concentrations (C_1, C_2) until the

error between successive iterations falls below a tolerance (10^{-9}) or the maximum iterations are reached.

$$L = \int_{\Omega} B^T B d\Omega \qquad M = \int_{\Omega} (B \cdot V) B^T \phi d\Omega \tag{25}$$

$$O = \int_{\Omega} \phi^T (\sum_{i=1}^{ns} z_i c_i) d\Omega \tag{26}$$

4. **Error Calculation:** For each refinement (number of nodes), compute the percentage errors in V, C_1, and C_2 by comparing the results with those obtained from the previous mesh refinement at specific checkpoints. Compute the common error as the sum of the individual percentage errors.

$$\begin{aligned} \text{Common} \quad \text{Error} = & \sum_{i=1}^{\text{checkpoints}} \frac{\|V[i] - V_{\text{prev}}[i]\|}{\|V_{\text{prev}}[i]\|} \\ & + \sum_{i=1}^{\text{checkpoints}} \frac{\|C1[i] - C1_{\text{prev}}[i]\|}{\|C1_{\text{prev}}[i]\|} \\ & + \sum_{i=1}^{\text{checkpoints}} \frac{\|C2[i] - C2_{\text{prev}}[i]\|}{\|C2_{\text{prev}}[i]\|} \end{aligned} \tag{27}$$

$$\text{Flux error} = \sum_{i=1}^{\text{checkpoints}} \frac{\|j[i] - j_{\text{prev}}[i]\|}{\|j_{\text{prev}}[i]\|} \tag{28}$$

5. **Visualization:** Plot the common error against the number of nodes to evaluate convergence behavior. The following table summarizes the percentage errors at specific checkpoints for each mesh refinement.

Table 2: Mesh convergence study: Percentage errors at checkpoints

Number of Nodes	**% Error in Primary Variables**	**% Error in Secondary Variable (Flux)**
15	0.0000000000	0.0000000000
100	11.7839810777	171.7180109565
500	2.0161142218	160.3206644028
750	0.2318892316	66.7556760016
1000	0.0804890534	50.0500507464
1250	0.1263198441	40.0320259633
1500	0.0403848065	33.3555705752
1750	0.0559821893	28.5877645552
2000	0.0410669685	25.0125063361
2250	0.0548274990	22.2321032144
2500	0.0241251576	20.0080032388

The rate of convergence for primary and Secondary varibales are as follows:-

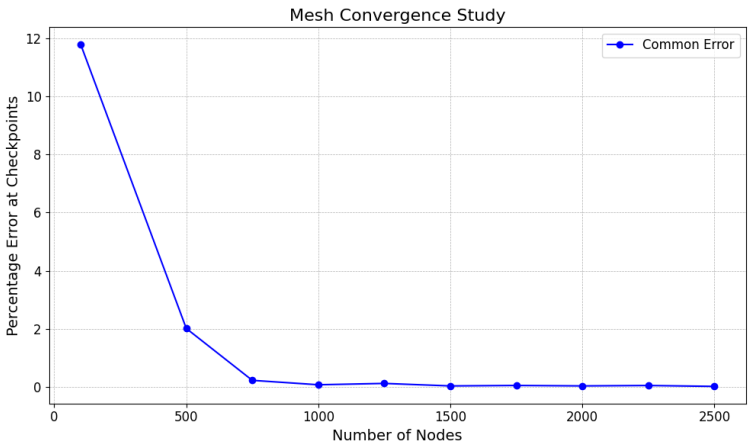

Figure 1: Mesh convergence study: Common error vs. number of nodes

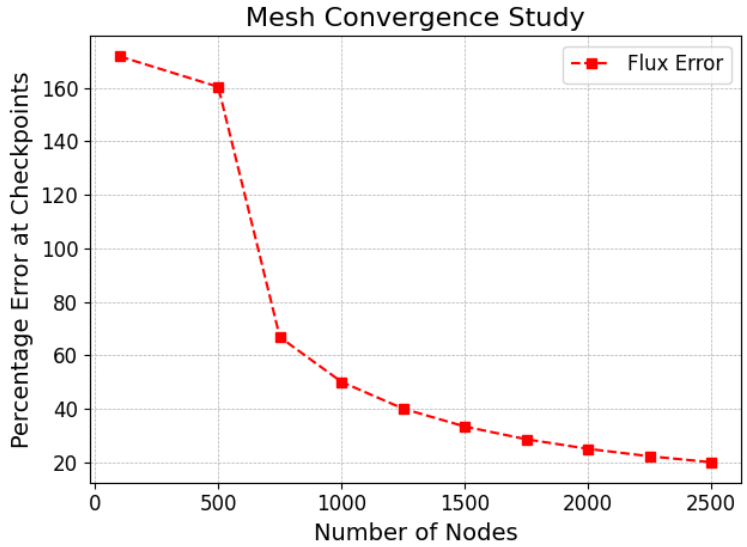

Figure 2: Mesh convergence study: Flux error vs. number of nodes

$$Rate\ of\ convergence\ for\ Primary\ variable = 1.97$$

$$Rate\ of\ convergence\ for\ Secondary\ variable = 1.2$$

8 Interpretation of results

To solve the NPP equations, we employed the Picard iteration method. The numerical examples are analyzed under the following four cases:

1) Behaviour with Charges $z_1 = 2$ and $z_2 = -1$

Observation: Species 2 (negatively charged) exhibits a maximum concentration somewhere in the middle, while Species 1 (positively charged) shows a minimum concentration also somewhere in the middle.

2) Behaviour with Charges $z_1 = 1$ and $z_2 = -2$

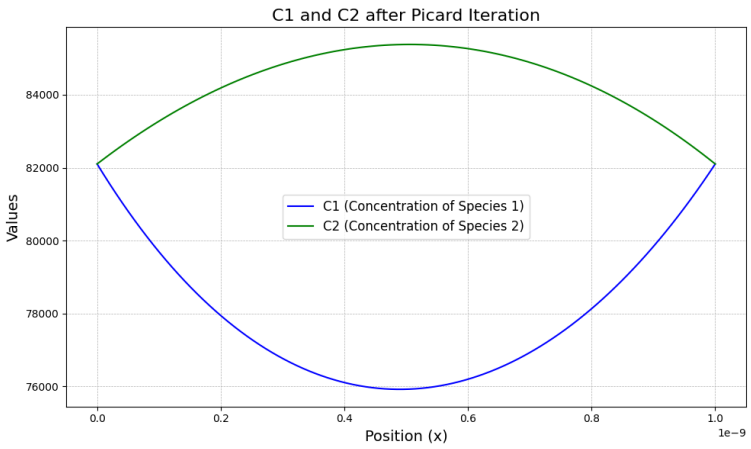

Figure 3: Concentration profiles for $z_1 = 2$ and $z_2 = -1$

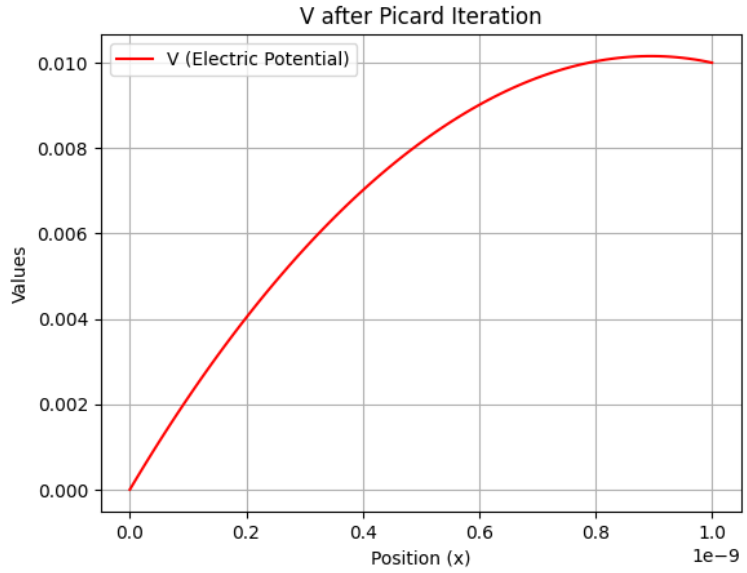

Figure 4: Voltage profiles for $V_{right} = 0.01$ and $V_{left} = 0$

Observation: The behavior is reversed: Species 1 (positively charged) now exhibits a maximum concentration in the middle, and Species 2 (negatively charged) shows a minimum concentration.

3) Effect of Changing V_{right} to 1 with $z_1 = 2$ and $z_2 = -1$ Observation: The maximum concentration of Species 2 (negatively charged) shifts towards the right, while the minimum concentration of Species 1 (positively charged) shifts towards the left.

4) Effect of Changing V_{right} to -1 with $z_1 = 2$ and $z_2 = -1$ Observation: The maxima of Species 2 shifts to the left, and the minima of Species 1 shifts to the right.

General Insights :

The interplay between the electric field (set by boundary conditions) and charge of species determines the movement of ions through electromigration.

Diffusion effects ensure that species also spread out to reduce concentration gradients, but the electric field can overcome diffusion to localize ions at specific regions.

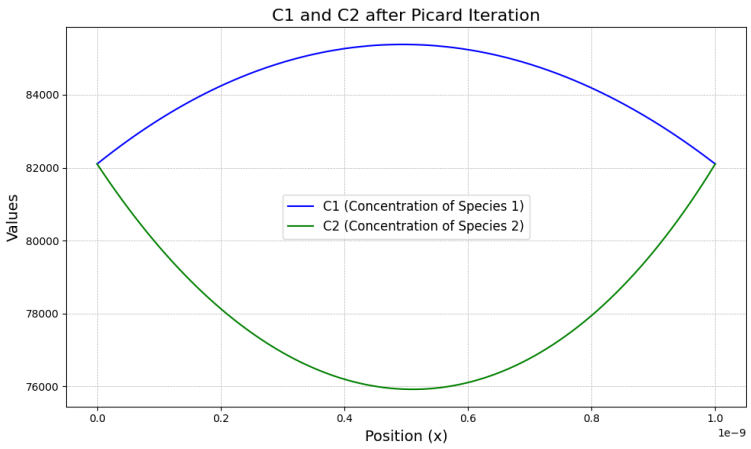

Figure 5: Concentration profiles for $z_1 = 1$ and $z_2 = -2$

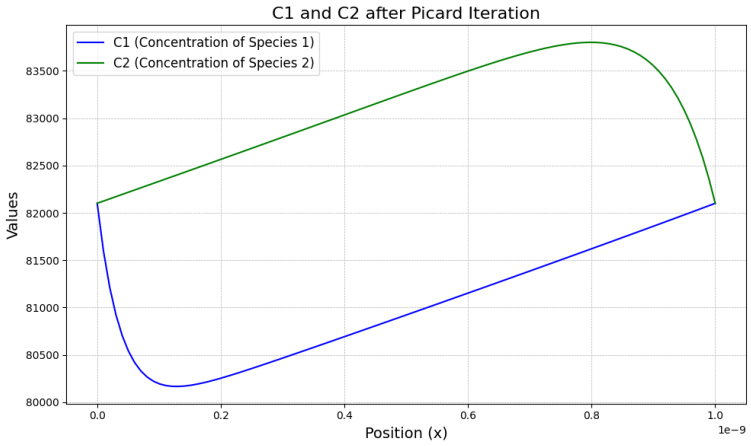

Figure 6: Voltage effect on concentration profiles for $z_1 = 2$ and $z_2 = -1$

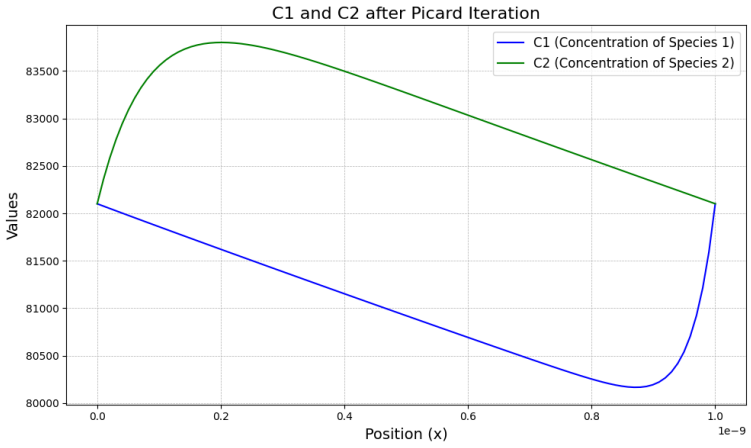

Figure 7: Voltage effect on concentration profiles for $z_1 = 2$ and $z_2 = -1$

The relative charge magnitudes influence the degree of repulsion or attraction, significantly altering the concentration profiles.

Boundary conditions for V_{left} and V_{right} control the direction and strength of the electric field, shifting the positions of maxima and minima accordingly.

9 Contributions

Yash Panasara (ME21B135): Led the conceptualization and literature review, implemented the numerical solution framework by deriving and assembling the L, M, and O matrices, and executed the Picard iteration process for solving the equations.

Jay Prajapati (ME21B143): Conducted the mesh convergence study to validate solution accuracy and robustness, generated visual plots to illustrate the results and trends effectively, and authored the comprehensive report detailing the methodology, results, and insights.

References

[1] P.A. Markowich, *Semiconductor Equations*, Springer-Verlag, Berlin, Heidelberg, 2012.

[2] J.W. Jerome, *Analysis of Charge Transport: A Mathematical Study of Semiconductor Devices*, 2012.

[3] G.-W. Wei, Q. Zheng, Z. Chen, K. Xia, *Variational multiscale models for charge transport*, SIAM Rev. 54 (4) (2012) 699-754.

[4] B. Eisenberg, W. Liu, *Poisson-Nernst-Planck systems for ion channels with permanent charges*, SIAM J. Math. Anal. 38 (6) (2007) 1932-1966.

[5] Q. Zheng, D. Chen, G.-W. Wei, *Second-order Poisson-Nernst-Planck solver for ion transport*, J. Comput. Phys. 230 (13) (2011) 5239-5262.

[6] R. Eisenberg, D. Chen, *Poisson-Nernst-Planck (PNP) theory of an open ionic channel*, Biophysical Journal Vol. 64, Biophysical Society 9650 Rockville Pike, Bethesda, MD 20814-3998, 1993. A22-A22.

[7] D.P. Chen, R.S. Eisenberg, J.W. Jerome, C.-W. Shu, *Hydrodynamic model of temperature change in open ionic channels*, Biophys. J. 69 (6) (1995) 2304-2322.

[8] V. Barcilon, D.-P. Chen, R. Eisenberg, *Ion flow through narrow membrane channels: part ii*, SIAM J. Appl. Math. 52 (5) (1992) 1405-1425.

[9] J.W. Jerome, *Consistency of semiconductor modeling: an existence/stability analysis for the stationary van Roosbroeck system*, SIAM J. Appl. Math. 45 (4) (1985) 565-590.

[10] N. Hayeck, A. Nachaoui, N.R. Nassif, *Existence and regularity for van Roosbroeck systems with general mixed boundary conditions*, COMPEL- Int. J. Comp. Math. Elect. Electr. Eng. 9 (4) (1990) 217-228.

[11] *Efficient numerical techniques for solving coupled Nernst-Planck-Poisson equations*, J. Nonlinear Sci., 2024.